Determination of self-diffusion mechanisms from high-field nuclear-spin-relaxation experiments

Dieter Wolf
Max-Planck-Institut für Metallforschung, Institut für Physik, Stuttgart, West Germany
(Received 11 March 1974)

The theory of high-field nuclear-spin relaxation due to random-walk diffusion in monoatomic crystals is extended to correlated diffusion mechanisms. It is predicted that the effect of the diffusion mechanism on the relaxation times T_1, T_2, and $T_{1\rho}$ can be observed in three different ways: (i) In single crystals the relaxation times are shown to depend on the crystallographic orientation of the magnetic field. Whereas on the low-temperature side of the T_1 minimum these anisotropies should characterize the diffusion mechanism, they are expected to disappear on the high-temperature side. (ii) Shape and width of the T_1 and $T_{1\rho}$ minimum as a function of temperature are found to depend on the diffusion mechanism—in both single crystals and polycrystalline samples. (iii) Assuming that in a single crystal the decay of the transverse magnetization can be described by a single relaxation time T_2 (usually true at temperatures above the T_1 minimum), deviations from the exponential decay, which should be characteristic for a given diffusion mechanism, are predicted in polycrystalline samples. The numerical results obtained for diffusion via monovacancies in bcc and fcc crystals are compared with those obtained for the limiting case of random-walk diffusion. It is found that for these two mechanisms the orientation dependences of the relaxation times are similar, but that considerable differences in the shapes of the relaxation rates versus temperature should exist.

I. INTRODUCTION

In most monoatomic crystals diffusion results from the migration of point defects (e.g., vacancies). Although these defects migrate randomly in the crystal lattice, successive jumps of atoms caused by the migration of these defects are in general not independent of each other, i.e., they are correlated.

For the study of diffusion by radioactive tracers these correlations are well understood. Since there we are concerned with the correlation of successive jump *directions* only, we speak of "spatial correlation."

Although originating from the same physical effect, the influence of correlations between successive jumps on nuclear magnetic relaxation is more complicated. Because in nuclear-magnetic-relaxation experiments there is an inherent time scale, the so-called "temporal correlation" enters here in addition to the spatial correlation. The temporal correlation takes into account that successive jumps of an atom caused by a randomly migrating defect are bunched into groups.

A qualitative description of the influence of correlations on the high-field nuclear magnetic relaxation was attempted by Eisenstadt and Redfield.[1] The present author[2] presented a quantitative treatment of correlated diffusion mechanisms (so-called "isotropic-vacancy model") based on Torrey's isotropic random-walk model of diffusion.[3] This treatment was unsatisfactory in two respects: (i) The basic theory, i.e., Torrey's random-walk model in isotropic solids, does not take into account the discrete structure of the crystal lattice in sufficient detail. As a consequence the theory describing correlated diffusion mechanisms[2] does not allow for single-crystal effects and is hence applicable to polycrystals only. (ii) The so-called "pair correlation" was neglected. While the correlations between the jumps of an individual spin were allowed for, it was assumed that successive jumps of two different spins (i.e., of a "spin pair") are not correlated with each other.

The purpose of the present paper is to remove these two restrictions and to develop a theory of nuclear spin relaxation by correlated diffusion mechanisms in crystals taking proper account of pair correlations.

Our starting point will be the theory of nuclear spin relaxation due to random-walk diffusion in crystals presented recently.[4] This theory allows for single crystal effects and avoids thus the first restriction.

II. BASIC THEORY

The density-matrix method generally applied to the calculation of the relaxation rates in the high-field region as described, e.g., by Abragam[5] is based on the applicability of perturbation theory. Although this method is restricted to uncorrelated relative motions of the nuclei it can easily be extended to include correlated relative motions, provided the correlation functions $G^{(q)}(t)$ are defined as

$$G^{(q)}(t)=\frac{1}{N}\sum_i\sum_m \langle F_{im}^{(q)}(t')F_{im}^{(q)*}(t'+t)\rangle_{t'}\,, \qquad (2.1)$$

where N is the number of nuclei in the crystal, and the geometrical functions $F_{im}^{(q)}(t)$ are defined as (see, e.g., Ref. 5)

$$F_{im}^{(0)} = r_{im}^{-3}(1 - 3\cos^2\theta_{im}) , \tag{2.2a}$$

$$F_{im}^{(1)} = r_{im}^{-3}\sin\theta_{im}\cos\theta_{im}\, e^{i\varphi_{im}} , \tag{2.2b}$$

$$F_{im}^{(2)} = r_{im}^{-3}\sin^2\theta_{im}\, e^{2i\varphi_{im}} . \tag{2.2c}$$

Here r_{im}, θ_{im}, and φ_{im} are the spherical coordinates of the vector $\vec{r}_{im}$ from spin i to spin m in a coordinate system with the strong external magnetic field H_0 parallel to the z axis. (For details see, e.g., Ref. 4.)

With definition (2.1), the equations for the relaxation rates $1/T_1$, $1/T_2$, and $1/T_{1\rho}$ can be written (see, e.g., Ref. 4) in terms of the spectral density functions

$$\mathcal{J}^{(q)}(\omega) = 2\int_0^\infty G^{(q)}(t)\, e^{i\omega t}\, dt \tag{2.3}$$

for both correlated and uncorrelated relative motions of the nuclei.

In order to introduce the microscopic features of the diffusion mechanism the time average in Eq. (2.1) is replaced by an ensemble average:

At $t = 0$, let spin m sit on the lattice site $\vec{r}_m^{\,0}$ and spin i on $\vec{r}_i^{\,0}$ relative to a common origin (see Fig. 1). The correlation of the jumps of m with those of i is assumed to be a function of the vector $\vec{r}_m^{\,0} - \vec{r}_i^{\,0}$ from spin i to spin m. During a time interval t both spins may jump, say, spin m to lattice site $\vec{r}_m$, spin i to $\vec{r}_i$. If $\vec{r}$ denotes the effective change of the initial relative vector $\vec{r}_m^{\,0} - \vec{r}_i^{\,0}$ during the interval t, the vector from i to m at time t is given by

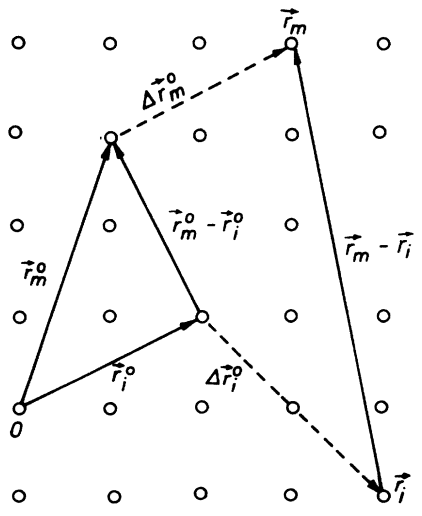

FIG. 1. Lattice plane of a primitive cubic lattice. Before the encounter spin i is located at the lattice site $\vec{r}_i^{\,0}$ relative to a common origin, spin m at $\vec{r}_m^{\,0}$. The sites of i and m after the encounter are denoted by $\vec{r}_i$ and $\vec{r}_m$, their displacement vectors by $\Delta\vec{r}_i^{\,0}$ and $\Delta\vec{r}_m^{\,0}$.

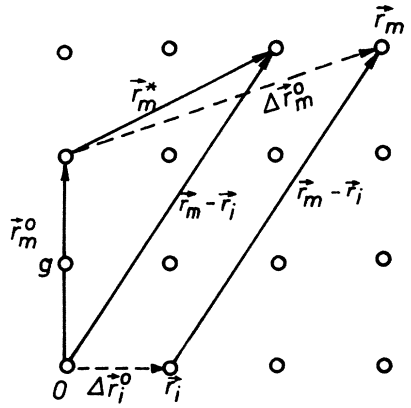

FIG. 2. Lattice plane of a primitive cubic lattice. Spin i is located at the origin, spin m at $\vec{r}_m^{\,0}$. The relative displacement of these two spins after the encounter may be characterized by the vector $\vec{r}_m^{\,*}$ (see also Sec. IV B). g denotes the nearest neighboring site, from which the vacancy initiates the first jump of spin i.

$$\vec{r}' = \vec{r}_m^{\,0} - \vec{r}_i^{\,0} + \vec{r} . \tag{2.4}$$

Defining $P(\vec{r}_m^{\,0} - \vec{r}_i^{\,0}, \vec{r}, t)$ as the probability that the change of the relative vector $\vec{r}_m^{\,0} - \vec{r}_i^{\,0}$ (at $t = 0$) during time t is equal to $\vec{r}$, we may write for the correlation function

$$G^{(q)}(t) = \frac{1}{N}\sum_{\vec{r}_i^{\,0}}\sum_{\vec{r}_m^{\,0}} F_{im}^{(q)}(\vec{r}_m^{\,0} - \vec{r}_i^{\,0}) \times \int_{\vec{r}} P(\vec{r}_m^{\,0} - \vec{r}_i^{\,0}, \vec{r}, t) F_{im}^{(q)*}(\vec{r}_m^{\,0} - \vec{r}_i^{\,0} + \vec{r})\, d^3r . \tag{2.5}$$

III. ENCOUNTER MODEL

In this section we introduce a model for correlated diffusion mechanisms which allows to replace the double sum in Eq. (2.5) by a single summation.

Let us consider a single vacancy entering the surroundings of the two spins i and m (indicated in Fig. 1). As the vacancy walks randomly through this region some nuclei will jump once or repeatedly; others will not. The result is a geometrical rearrangement of the atoms. Let us assume that i is the only spin about which we know for sure that it jumped at least once during the rearrangement. Any other nucleus in the neighborhood of spin i may have jumped with a certain conditional probability. Since these jumps were caused by the same vacancy they are correlated with the jumps of spin i. As first suggested by Eisenstadt and Redfield, [1] the entire rearrangement is called an "encounter" of spin i with the vacancy. An encounter thus consists of a number of relative jumps of the atoms caused by the same vacancy.

Since for the usual vacancy concentrations (typically about 10^{-4}–10^{-7}) the rearrangements due to different vacancies are independent of each other,

the encounter of spin i described above may be looked upon as representative for any rearrangement due to any vacancy.

The statistical description of the encounter of spin i (from now on assumed to be located at the origin in Fig. 1, see Fig. 2) starts from the fact that the entire rearrangement due to an encounter depends on the nearest-neighbor site g ($g = 1, \ldots, G$; G is the number of nearest neighbors in the crystal lattice) from which the vacancy jumps into the origin and, thus, causes the first jump of i. The probability that a spin m, originally at $\vec{r}_m^0$, will be located at $\vec{r}_m$ after the encounter is denoted by $B_g(\vec{r}_m^0, \vec{r}_m)$. Similarly, the probabilities for spin i are denoted by $B_g(0, \vec{r}_i)$ (see Fig. 2). Thus, we have

$$\sum_{\vec{r}_m} B_g(\vec{r}_m^0, \vec{r}_m) = 1 \tag{3.1a}$$

and

$$\sum_{\vec{r}_i} B_g(0, \vec{r}_i) = 1 \,, \tag{3.1b}$$

where the sums extend over all lattice points.

The mean number of correlated jumps of m during the encounter of i, $Z(\vec{r}_m^0)$, depends on g. Thus, we write

$$Z(\vec{r}_m^0) = \frac{1}{G} \sum_{g=1}^{G} Z_g(\vec{r}_m^0) \,, \tag{3.2}$$

where $Z_g(\vec{r}_m^0)$ denotes the number of jumps of m if the initial jump of i ends on the nearest neighbor site g. The mean number of jumps of spin i during an encounter is denoted by $Z(0)$.

The quantities $B_g(\vec{r}_m^0, \vec{r}_m)$ and $Z(\vec{r}_m^0)$ (including $\vec{r}_m^0 = 0$) defined above as averages over a great number of encounters are the only parameters entering into the statistical description of an encounter. They must be calculated numerically for a given diffusion mechanism.

As mentioned above, for small vacancy concentrations different encounters are independent of each other. Therefore, the relative displacement of i and m due to a random sequence of encounters with different vacancies may be determined similarly as in the random-walk model of diffusion, which deals with a random sequence of individual jumps to nearest-neighbor sites.[4] The only difference is that the "random walk of encounters" allows the individual displacements per encounter to be different from the vectors to the nearest neighbor sites and to consist of more than only one jump.

The mean time τ_{NMR} between two encounters must be distinguished from the mean time τ of stay of an atom at a lattice site, which is defined via the coefficient of self-diffusion D^{SD} by the Einstein relation

$$D^{\mathrm{SD}} = \langle r^2 \rangle / 6\tau \,, \tag{3.3}$$

where $\langle r^2 \rangle$ denotes the mean square of the jump distance.

The number of relative jumps of i and m in an encounter of spin i is $Z(0) + Z(\vec{r}_m^0)$. In an encounter of m spin i jumps $Z(-\vec{r}_m^0)$ times on the average. Since $Z(\vec{r}_m^0) = Z(-\vec{r}_m^0)$ we can write for the rate of encounters of the two spins

$$1/\tau_{\mathrm{NMR}} = (2/\tau)[Z(0) + Z(\vec{r}_m^0)]^{-1} \tag{3.4}$$

The analogy between a random-walk diffusion mechanism and correlated diffusion mechanisms, which is based on the fact that the encounter of spin i as described above is taken as representative of the encounters of any spin, allows us to simplify Eq. (2.5). Replacing the summation over i by a multiplying factor N, we obtain

$$G^{(q)}(t) = \sum_{\vec{r}_m^0} F_{im}^{(q)}(\vec{r}_m^0) \int_{\vec{r}} P(\vec{r}_m^0, \vec{r}, t) \times F_{im}^{(q)*}(\vec{r}_m^0 + \vec{r}) d^3r \,. \tag{3.5}$$

This correlation function is formally identical with that obtained in Ref. 4 for random-walk diffusion. The characteristics of a given diffusion mechanism enter into the probabilities $P(\vec{r}_m^0, \vec{r}, t)$.

IV. RECURSIVE CALCULATION OF SPECTRAL-DENSITY FUNCTIONS

A. Basic relations

For the calculation of the probabilities $P(\vec{r}_m^0, \vec{r}, t)$ for the spin pair i-m we first separate the time scale from the geometrical properties by means of the relation (see, e.g., Refs. 4 and 3)

$$P(\vec{r}_m^0, \vec{r}, t) = \sum_{s=0}^{\infty} w_s(t, \tau_{\mathrm{NMR}}^{(s)}) P_s(\vec{r}_m^0, \vec{r}) \,. \tag{4.1}$$

$P_s(\vec{r}_m^0, \vec{r})$ denotes the conditional probability that after s encounters the vector from i to m is $\vec{r}_m^0 + \vec{r}$ if it was $\vec{r}_m^0$ at $t = 0$. $w_s(t, \tau_{\mathrm{NMR}}^{(s)})$ denotes the probability that s encounters occur during the time interval t. The dependence of $\tau_{\mathrm{NMR}}^{(s)}$ on s originates from the fact that the vector from i to m (which is a measure for the degree of correlation of the jumps of m with those of i) changes with time. Thus, both the mean number of relative jumps per encounter and τ_{NMR} [see Eq. (3.4)] vary from encounter to encounter.

If $\overline{Z}_{\mathrm{NMR}}^{(s)}$ denotes the mean number of relative jumps of i and m averaged arithmetically over s encounters, we may define in analogy to Eq. (3.4),

$$1/\tau_{\mathrm{NMR}}^{(s)} = (2/\tau) 1/\overline{Z}_{\mathrm{NMR}}^{(s)} \,. \tag{4.2}$$

For the usual vacancy concentrations (see Sec. III) the mean time between two encounters is long compared with the time interval, during which the vacancy rearranges the surroundings of spin i.

Therefore, we may use a Poisson distribution for $w_s(t, \tau_{\mathrm{NMR}}^{(s)})$:

$$w_s(t, \tau_{\mathrm{NMR}}^{(s)}) = \frac{1}{s!}\left(\frac{t}{\tau_{\mathrm{NMR}}^{(s)}}\right)^s \exp\left(-\frac{t}{\tau_{\mathrm{NMR}}^{(s)}}\right) \tag{4.3}$$

From Eq. (4.3) we may calculate the probability that no encounter occurs in time t by means of the relation

$$w_0(t, \tau_{\mathrm{NMR}}^{(s)}) = 1 - \sum_{s=1}^{\infty} w_s(t, \tau_{\mathrm{NMR}}^{(s)}) \ . \tag{4.4}$$

Since the nuclei diffuse on a discrete crystal lattice, the vector $\vec{r}$ is a discrete lattice vector after an arbitrary number of encounters. Hence we may write similarly as in Ref. 4,

$$P_s(\vec{r}_m^{\,0}, \vec{r}) = \sum_{\vec{r}_m^{\,*}} W_s(\vec{r}_m^{\,0}, \vec{r}_m^{\,*})\delta(\vec{r} - \vec{r}_m^{\,*}) \tag{4.5}$$

including

$$P_0(\vec{r}_m^{\,0}, \vec{r}) = \delta(\vec{r}) \ . \tag{4.6}$$

$W_s(\vec{r}_m^{\,0}, \vec{r}_m^{\,*})$ denotes the probability that after s encounters the vector from i to m is equal to $\vec{r}_m^{\,0} + \vec{r}_m^{\,*}$, where $\vec{r}_m^{\,*}$ may be any vector allowed by the crystal structure.

Inserting Eqs. (4.5) and (4.6) into (4.1), we get

$$P(\vec{r}_m^{\,0}, \vec{r}, t) = w_0(t, \tau_{\mathrm{NMR}}^{(s)})\delta(\vec{r}) + \sum_{s=1}^{\infty}\sum_{\vec{r}_m^{\,*}} w_s(t, \tau_{\mathrm{NMR}}^{(s)}) W_s(\vec{r}_m^{\,0}, \vec{r}_m^{\,*})\delta(\vec{r} - \vec{r}_m^{\,*}) \ . \tag{4.7}$$

B. Recursive calculation of the quantities depending on diffusion mechanism

The probabilities $W_1(\vec{r}_m^{\,0}, \vec{r}_m^{\,*})$ may be related to the probabilities $B_g(0, \vec{r}_i)$ and $B_g(\vec{r}_m^{\,0}, \vec{r}_m)$ defined in Sec. III. Averaging over all nearest-neighbor positions from which the vacancy may jump into the origin, we find

$$W_1(\vec{r}_m^{\,0}, \vec{r}_m^{\,*}) = \frac{1}{G}\sum_{g=1}^{G}\sum_{\vec{r}_i}{}'\sum_{\vec{r}_m}{}' B_g(0, \vec{r}_i) B_g(\vec{r}_m^{\,0}, \vec{r}_m) \ , \tag{4.8}$$

where the double summation over $\vec{r}_i$ and $\vec{r}_m$ is restricted by the relation (see Fig. 2)

$$\vec{r}_m^{\,0} + \vec{r}_m^{\,*} = \vec{r}_m - \vec{r}_i \ . \tag{4.9}$$

Inserting Eq. (4.9) into (4.8), we get

$$W_1(\vec{r}_m^{\,0}, \vec{r}_m^{\,*}) = \frac{1}{G}\sum_{g=1}^{G}\sum_{\vec{r}_i} B_g(0, \vec{r}_i) B_g(\vec{r}_m^{\,0}, \vec{r}_m^{\,0} + \vec{r}_m^{\,*} + \vec{r}_i) \ . \tag{4.10a}$$

It is obvious that the relationship

$$\sum_{\vec{r}_m^{\,*}} W_1(\vec{r}_m^{\,0}, \vec{r}_m^{\,*}) = 1 \tag{4.10b}$$

must hold for each vector $\vec{r}_m^{\,0}$. Analogously to the method described in Ref. 4 the probabilities $W_s(\vec{r}_m^{\,0}, \vec{r}_m^{\,*})$ may be calculated from the recursion formula

$$W_s(\vec{r}_m^{\,0}, \vec{r}_m^{\,*}) = \sum_{\vec{r}^{\,*}}\sum_{\vec{r}_1} W_{s-1}(\vec{r}_m^{\,0}, \vec{r}^{\,*}) W_1(\vec{r}_m^{\,0} + \vec{r}^{\,*}, \vec{r}_1) \ . \tag{4.11}$$

The vectors entering into Eq. (4.11) are defined in Fig. 3, which also shows that the double summation over $\vec{r}^{\,*}$ and $\vec{r}_1$ has to be performed under the restriction

$$\vec{r}_m^{\,*} = \vec{r}^{\,*} + \vec{r}_1 \ . \tag{4.12}$$

Substituting Eq. (4.12) into (4.11), we obtain

$$W_s(\vec{r}_m^{\,0}, \vec{r}_m^{\,*}) = \sum_{\vec{r}^{\,*}} W_{s-1}(\vec{r}_m^{\,0}, \vec{r}^{\,*}) W_1(\vec{r}_m^{\,0} + \vec{r}^{\,*}, \vec{r}_m^{\,*} - \vec{r}^{\,*}) \ . \tag{4.13}$$

What remains for the final evaluation of $P(\vec{r}_m^{\,0}, \vec{r}, t)$ from Eq. (4.7) is the calculation of the number of relative jumps $\overline{Z}_{\mathrm{NMR}}^{(s)}$ averaged over s successive encounters [see Eq. (4.2)].

For $s = 1$, we have

$$\overline{Z}_{\mathrm{NMR}}^{(1)} = Z(0) + Z(\vec{r}_m^{\,0}) \ . \tag{4.14}$$

The total number of relative jumps in the first $(s-1)$ encounters is (from the definition of $\overline{Z}_{\mathrm{NMR}}^{(s)}$) equal to $(s-1)\overline{Z}_{\mathrm{NMR}}^{(s-1)}$. The number of relative jumps in the next encounter (number s) is equal to $Z(0) + Z(\vec{r}_m^{\,0} + \vec{r}^{\,*})$, provided the vector from i to m is $\vec{r}_m^{\,0} + \vec{r}^{\,*}$ after $s-1$ encounters. Then we may write

$$\overline{Z}_{\mathrm{NMR}}^{(s)} = \frac{1}{s}\left((s-1)\overline{Z}_{\mathrm{NMR}}^{(s-1)} + Z(0) + \sum_{\vec{r}^{\,*}} W_{s-1}(\vec{r}_m^{\,0}, \vec{r}^{\,*}) Z(\vec{r}_m^{\,0} + \vec{r}^{\,*})\right) \ . \tag{4.15}$$

Since in every encounter one of the two spins of the couple jumps $Z(0)$ times on the average, we may write for $\overline{Z}_{\mathrm{NMR}}^{(s)}$:

$$\overline{Z}_{\mathrm{NMR}}^{(s)} = Z(0)[1 + \Delta(s)] \ , \tag{4.16}$$

where an equation for $\Delta(s)$ may be derived by comparison of Eq. (4.16) with (4.15), e.g.,

$$\Delta(1) = Z(\vec{r}_m^{\,0})/Z(0) \ . \tag{4.17}$$

$\Delta(s)$ is a measure of the pair correlation, i.e., a

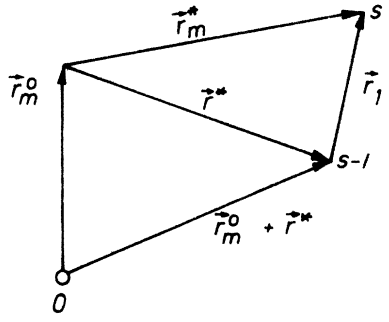

FIG. 3. Before the first encounter spin i is located at the origin, spin m at $\vec{r}_m^{\,0}$. The relative displacement vector after one encounter is denoted by $\vec{r}_1$, after s-1 encounters by $\vec{r}^{\,*}$, and after s encounters by $\vec{r}_m^{\,*}$.

measure for the motions of spin m induced in an encounter of spin i. The influence of pair correlations on the spectral density functions (deduced in Sec. IV C) as a function of the initial vector $\vec{r}_m^{\,0}$ or the number of encounters s may be studied in terms of the variation of $\Delta(s)$ with $\vec{r}_m^{\,0}$ or s.

C. Calculation of the correlation functions

With the results of Sec. IV B we are now able to calculate the correlation functions for correlated relative motions of the spins. Inserting Eqs. (4.3), (4.2), and (4.16) into (4.4), we obtain

$$w_0(t, \tau_{\mathrm{NMR}}^{(s)}) = 1 - \sum_{s=1}^{\infty} \frac{1}{s!} \frac{(t/\tau_0)^s}{[1+\Delta(s)]^s} \exp\left(-\frac{t/\tau_0}{1+\Delta(s)}\right), \tag{4.18}$$

where, making use of Eqs. (4.16) and (4.2), $\tau_{\mathrm{NMR}}^{(s)}$ was replaced by

$$\tau_{\mathrm{NMR}}^{(s)} = \tau_0[1+\Delta(s)] , \tag{4.19}$$

with

$$\tau_0 = \tfrac{1}{2}\tau Z(0) . \tag{4.20}$$

Neglecting the change of the pair correlation with the number of encounters, i.e., substituting

$$\Delta(s) = \Delta(1) \tag{4.21}$$

into (4.18), we obtain to a good approximation

$$w_0(t, \tau_{\mathrm{NMR}}^{(s)}) = \exp\left(-\frac{t}{\tau_{\mathrm{NMR}}^{(1)}}\right) . \tag{4.22}$$

Now, $P(\vec{r}_m^{\,0}, \vec{r}, t)$ may be calculated. From Eqs. (4.22) and (4.7), we obtain

$$P(\vec{r}_m^{\,0}, \vec{r}, t) = \exp\left(-\frac{t}{\tau_{\mathrm{NMR}}^{(1)}}\right)\delta(\vec{r}) + \sum_{s=1}^{\infty} \frac{1}{s!}\left(\frac{t}{\tau_{\mathrm{NMR}}^{(s)}}\right)^s \times \exp\left(-\frac{t}{\tau_{\mathrm{NMR}}^{(s)}}\right) \sum_{\vec{r}_m^{\,*}} W_s(\vec{r}_m^{\,0}, \vec{r}_m^{\,*})\delta(\vec{r} - \vec{r}_m^{\,*}) . \tag{4.23}$$

From Eqs. (4.23) and (3.5) we obtain, for the correlation function,

$$G^{(q)}(t) = \sum_{\vec{r}_m^{\,0}} |F_{im}^{(q)}(\vec{r}_m^{\,0})|^2 \exp\left(-\frac{t}{\tau_{\mathrm{NMR}}^{(1)}}\right) + \sum_{s=1}^{\infty} \sum_{\vec{r}_m^{\,0}} \frac{1}{s!}\left(\frac{t}{\tau_{\mathrm{NMR}}^{(s)}}\right)^s \exp\left(-\frac{t}{\tau_{\mathrm{NMR}}^{(s)}}\right) F_{im}^{(q)}(\vec{r}_m^{\,0}) \sum_{\vec{r}_m^{\,*}} F_{im}^{(q)*}(\vec{r}_m^{\,0} + \vec{r}_m^{\,*}) W_s(\vec{r}_m^{\,0}, \vec{r}_m^{\,*}) , \tag{4.24}$$

and from Eq. (2.4)

$$\mathcal{J}^{(q)}(\omega) = \frac{1}{\omega}\left(\sum_{\vec{r}_m^{\,0}} |F_{im}^{(q)}(\vec{r}_m^{\,0})|^2 j_0(\omega\tau_{\mathrm{NMR}}^{(1)}) + \sum_{s=1}^{\infty} \sum_{\vec{r}_m^{\,0}} j_s(\omega\tau_{\mathrm{NMR}}^{(s)}) F_{im}^{(q)}(\vec{r}_m^{\,0}) \sum_{\vec{r}_m^{\,*}} F_{im}^{(q)*}(\vec{r}_m^{\,0} + \vec{r}_m^{\,*}) W_s(\vec{r}_m^{\,0}, \vec{r}_m^{\,*})\right) , \tag{4.25}$$

with (see Ref. 4)

$$j_s(x) = \mathrm{Re}\left(\frac{2x}{(1-ix)^{s+1}}\right) = \frac{2x}{(1+x^2)^{s+1}} \sum_{n=0}^{K} (-1)^n \binom{s+1}{2n} x^{2n} , \tag{4.26}$$

where $x = \omega\tau_{\mathrm{NMR}}^{(s)}$ and K is the greatest integer $\leq (s+1)/2$. In Eqs. (4.24) and (4.25) it must not be forgotten that $\tau_{\mathrm{NMR}}^{(s)}$ depends on $\vec{r}_m^{\,0}$ [see Eqs. (4.19) and (4.47)]. Therefore, $j_s(\omega\tau_{\mathrm{NMR}}^{(s)})$ depends on $\vec{r}_m^{\,0}$ also.

The spectral density functions (4.25) describe the relaxation behavior due to a correlated diffusion mechanism in single crystals. Before we start with the numerical evaluation of $\mathcal{J}^{(q)}(\omega)$ from Eq. (4.25) we shall compare the case of uncorrelated random-walk diffusion, contained in Eq. (4.25) as a limiting case, with the results obtained recently.[4]

V. SPECIAL CASE OF UNCORRELATED RANDOM-WALK DIFFUSION

Neglecting both pair correlations and the correlation of successive jumps of spin i, the encounter of spin i is reduced to a single jump of spin i to a nearest-neighbor site.

We may then write

$$B_g(0, \vec{r}_i) = (1/G)\delta_{\vec{r}_i, \vec{r}_g} \tag{5.1a}$$

and

$$B_g(\vec{r}_m^{\,0}, \vec{r}_m) = \delta_{\vec{r}_m, \vec{r}_m^{\,0}} , \tag{5.1b}$$

where $\delta_{\vec{r}_m, \vec{r}_m^{\,0}}$ denotes the Kronecker symbol which is 1 for $\vec{r}_m^{\,0} = \vec{r}_m$, and 0 otherwise). With Eqs. (5.1) we obtain, from Eq. (4.8),

$$W_1(\vec{r}_m^{\,0}, \vec{r}_m^{\,*}) \equiv W_1(\vec{r}_m^{\,*}) = \frac{1}{G}\delta_{\vec{r}_m^{\,*}, \vec{r}_g} , \tag{5.2}$$

where $\vec{r}_g$ ($g = 1, \ldots, G$) denotes the vectors from spin i to the G nearest-neighboring sites in the crystal lattice.

Similarly, we get, from Eq. (4.11),

$$W_s(\vec{r}_m^{\,0}, \vec{r}_m^{\,*}) \equiv W_s(\vec{r}_m^{\,*}) = \frac{1}{G}\sum_{\vec{r}^{\,*}} W_{s-1}(\vec{r}^{\,*})\delta_{\vec{r}_m^{\,*}, \vec{r}^{\,*}+\vec{r}_g} . \tag{5.3}$$

For uncorrelated diffusion the number of encounters per second is replaced by the number of relative jumps per second. With $\bar{Z}_{\mathrm{NMR}}^{(s)} = 1$, we obtain, from Eq. (4.2),

$$1/\tau_{\mathrm{NMR}}^{(s)} \equiv 1/\tau_{\mathrm{NMR}} = 2/\tau . \tag{5.4}$$

Substituting Eq. (5.4) and (5.3) into (4.25), we get

$$\mathcal{J}^{(q)}(\omega)=\frac{1}{\omega}\sum_{\vec{r}_m^0} F_{im}^{(q)}(\vec{r}_m^0)\sum_{s=0}^{\infty}\sum_{\vec{r}_m^*} W_s(\vec{r}_m^*) \times F_{im}^{(q)*}(\vec{r}_m^0+\vec{r}_m^*)\,j_s(\omega\tau)\,, \qquad (5.5)$$

with $j_s(x)$ given by Eq. (4.21) with $x=\frac{1}{2}\omega\tau$ (independent of $\vec{r}_m^0$). Equations (5.5) and (5.3) are identical with the relations derived for random walk diffusion in single crystals.[4] As shown in Ref. 4, Eq. (5.5) is in agreement with the relation found by Torrey[2] based on the theory of random flights.

VI. HOW TO DISTINGUISH BETWEEN DIFFERENT DIFFUSION MECHANISMS

The encounter concept is not limited to a monovacancy mechanism but may as well be applied to any kind of rearrangement due to randomly migrating point defects, like, e.g., for the divacancy, the interstitial, or the interstitialcy mechanism of self-diffusion. As shown in Sec. V, even a random-walk mechanism may be understood in terms of the encounter model. Equation (4.25) is thus valid for any point-defect mechanism of self-diffusion in crystals, which is characterized by the quantities $Z(\vec{r}_m^0)$ and $W_1(\vec{r}_m^0, \vec{r}_m^*)$.

A. Single crystals

In order to see the effect of different diffusion mechanisms on the spectral density functions $\mathcal{J}^{(q)}(\omega)$, Eq. (4.25) is rewritten using the procedure for the evaluation of lattice sums described in Ref. 4. There it was found that

$$\mathrm{Re}\{F_{im}^{(q)}(\vec{r}_m^0)F_{im}^{(q)*}(\vec{r}_m)\}=A^{(q)}+B^{(q)}\sin^2 2\theta + C^{(q)}\sin^4\theta\sin^2 2\phi\,, \qquad (6.1)$$

where $A^{(q)}$, $B^{(q)}$, and $C^{(q)}$ are functions of the crystallographic coordinates of the vectors $\vec{r}_m^0$ and $\vec{r}_m$, and the angles θ and ϕ characterize the crystallographic orientation of the magnetic field (see Ref. 4). Substituting Eq. (6.1) into (4.25), we get

$$\mathcal{J}_{(\omega)}^{(q)}=\frac{1}{\omega}\sum_m\sum_{s=0}^{\infty} j_s(\omega\tau_{\mathrm{NMR}}^{(s)})[A_m^{(q)}(s)+B_m^{(q)}(s)\sin^2 2\theta + C_m^{(q)}(s)\sin^4\theta\sin^2 2\phi]\,, \qquad (6.2)$$

with

$$A_m^{(q)}(s)=\sum_{\vec{r}_m^*} W_s(\vec{r}_m^0,\vec{r}_m^*)A^{(q)}\,, \qquad (6.3a)$$

$$B_m^{(q)}(s)=\sum_{\vec{r}_m^*} W_s(\vec{r}_m^0,\vec{r}_m^*)B^{(q)}\,, \qquad (6.3b)$$

$$C_m^{(q)}(s)=\sum_{\vec{r}_m^*} W_s(\vec{r}_m^0,\vec{r}_m^*)C^{(q)}\,. \qquad (6.3c)$$

Taking into account that for all m-spins located on the same atomic shell around spin i $Z_{\mathrm{NMR}}^{(s)}$ accepts the same values it is found from Eq. (4.2) and the definitions of $B^{(q)}$ and $C^{(q)}$ in Ref. 4 that for an arbitrary value of the parameter $\omega\tau$ we have

$$\sum_m j_s(\omega\tau_{\mathrm{NMR}}^{(s)})B_m^{(q)}(s)=\sum_m j_s(\omega\tau_{\mathrm{NMR}}^{(s)})C_m^{(q)}(s)\,. \qquad (6.4)$$

Substituting Eq. (6.4) into (6.2), we get

$$\mathcal{J}_{(\omega)}^{(q)}=\frac{1}{\omega}\sum_m\sum_{s=0}^{\infty} j_s(\omega\tau_{\mathrm{NMR}}^{(s)})[A_m^{(q)}(s)+f(\theta,\phi)B_m^{(q)}(s)]\,, \qquad (6.5)$$

where

$$f(\theta,\phi)=\sin^2 2\theta+\sin^4\theta\sin^2 2\phi\,. \qquad (6.6)$$

Analogously to the procedure described in Ref. 4, we obtain, for $\omega\tau\gg 1$,

$$\mathcal{J}_{(\omega)}^{(q)}=\frac{4}{\omega^2\tau}\left(\sum_m \frac{[A_m^{(q)}(0)-A_m^{(q)}(1)]}{\bar{Z}_{\mathrm{NMR}}^{(1)}} + f(\theta,\phi)\sum_m \frac{[B_m^{(q)}(0)-B_m^{(q)}(1)]}{\bar{Z}_{\mathrm{NMR}}^{(1)}}\right) \qquad (6.7)$$

and for $\omega\tau\ll 1$,

$$\mathcal{J}_{(\omega)}^{(q)}=\tau\left(\sum_m\sum_{s=0}^{\infty} A_m^{(q)}(s)\bar{Z}_{\mathrm{NMR}}^{(s)} + f(\theta,\phi)\sum_m\sum_{s=0}^{\infty} B_m^{(q)}(s)\bar{Z}_{\mathrm{NMR}}^{(s)}\right). \qquad (6.8)$$

The spectral density functions (6.5) enable us to calculate the high-field relaxation rates from the relationships

$$1/T_1=\tfrac{3}{2}\gamma^4\hbar^2 I(I+1)[\mathcal{J}^{(1)}(\omega_0)+\mathcal{J}^{(2)}(2\omega_0)]\,, \qquad (6.9a)$$

$$1/T_2=\tfrac{3}{8}\gamma^4\hbar^2 I(I+1) \times[\mathcal{J}^{(0)}(0)+10\,\mathcal{J}^{(1)}(\omega_0)+\mathcal{J}^{(2)}(2\omega_0)]\,, \qquad (6.9b)$$

$$1/T_{1\rho}=\tfrac{3}{8}\gamma^4\hbar^2 I(I+1) \times[\mathcal{J}^{(0)}(2\omega_1)+10\,\mathcal{J}^{(1)}(\omega_0)+\mathcal{J}^{(2)}(2\omega_0)]\,. \qquad (6.9c)$$

Here $\omega_0=\gamma H_0$ and $\omega_1=\gamma H_1$. The restriction of (6.9) to high fields requires the conditions $H_0\gg H_L$ (in the laboratory frame) or $H_1\gg H_{L\rho}$ (in the rotating frame) to hold, where H_L and $H_{L\rho}$ denote the local fields in the laboratory and rotating frame, respectively. H_1 denotes the amplitude of the rf field rotating around the direction of $\vec{H}_0$.

1. Orientation dependence of relaxation times

For a given value of $\omega\tau$ the dependence of the relaxation rates (6.9) on the crystallographic orientation of the magnetic field is determined by the factors $A_m^{(q)}(s)$ and $B_m^{(q)}(s)$, which depend on the diffusion mechanism [see Eqs. (6.3)].

In the following three temperature ranges, the orientation dependence can be readily obtained from Eqs. (6.7) to (6.9):

(i) $\omega_0\tau \ll 1$, $\omega_1\tau \ll 1$ ("high-temperature region," i.e., high-temperature side of the T_1-minimum):

$$\frac{1}{T_1} = \tfrac{3}{2}\gamma^4\hbar^2 I(I+1)\,\tau \sum_s \sum_m [A_m^{(1)}(s) + A_m^{(2)}(s)]\,\overline{Z}_{\mathrm{NMR}}^{(s)}, \tag{6.10a}$$

$$\frac{1}{T_2} = \tfrac{3}{8}\gamma^4\hbar^2 I(I+1)\,\tau \sum_s \sum_m [A_m^{(0)}(s) + 10A_m^{(1)}(s) + A_m^{(2)}(s)]\,\overline{Z}_{\mathrm{NMR}}^{(s)}, \tag{6.10b}$$

$$\frac{1}{T_{1\rho}} = \tfrac{3}{8}\gamma^4\hbar^2 I(I+1)\,\tau \sum_s \sum_m [A_m^{(0)}(s) + 10A_m^{(1)}(s) + A_m^{(2)}(s)]\,\overline{Z}_{\mathrm{NMR}}^{(s)}. \tag{6.10c}$$

From Eqs. (6.10a)–(6.10c) the relaxation times are predicted to be independent of the crystallographic orientation of the magnetic field. In addition, in this temperature range $T_{1\rho}$ is expected to be equal to T_2. So far, the more general relationship

$$T_1 = T_2 = T_{1\rho} \tag{6.11}$$

could not be derived analytically in terms of the encounter concept for arbitrary diffusion mechanism. Numerically, however, Eq. (6.11) was found to be valid for a random-walk mechanism of diffusion[4] and for diffusion via single vacancies (see Sec. VII B).

(ii) $\omega_0\tau \gg 1$, $\omega_1\tau \ll 1$ ("medium-temperature region," i.e., low-temperature side of the T_1 minimum, high-temperature side of the $T_{1\rho}$ minimum):

$$\frac{1}{T_1} = \tfrac{3}{2}\gamma^4\hbar^2 I(I+1)\,\frac{1}{\omega_0^2\tau}\left(\sum_m \frac{4A_m^{(1)}(0) - 4A_m^{(1)}(1) + A_m^{(2)}(0) - A_m^{(2)}(1)}{\overline{Z}_{\mathrm{NMR}}^{(1)}} + f(\theta,\phi)\sum_m \frac{3[B_m^{(1)}(0) - B_m^{(1)}(1)]}{\overline{Z}_{\mathrm{NMR}}^{(1)}}\right), \tag{6.12a}$$

$$\frac{1}{T_2} = \tfrac{3}{8}\gamma^4\hbar^2 I(I+1)\tau\left(\sum_s \sum_m A_m^{(0)}(s)\,\overline{Z}_{\mathrm{NMR}}^{(s)} + f(\theta,\phi)\sum_s \sum_m B_m^{(0)}(s)\,\overline{Z}_{\mathrm{NMR}}^{(s)}\right), \tag{6.12b}$$

$$\frac{1}{T_{1\rho}} = \tfrac{3}{8}\gamma^4\hbar^2 I(I+1)\tau\left(\sum_s \sum_m A_m^{(0)}(s)\,\overline{Z}_{\mathrm{NMR}}^{(s)} + f(\theta,\phi)\sum_s \sum_m B_m^{(0)}(s)\,\overline{Z}_{\mathrm{NMR}}^{(s)}\right). \tag{6.12c}$$

As we see from these equations, T_1, T_2, and $T_{1\rho}$ are expected to be orientation dependent for medium temperatures, and $T_{1\rho}$ should be identical with T_2.

(iii) $\omega_0\tau \gg 1$, $\omega_1\tau \gg 1$ ("low-temperature region," i.e., low-temperature side of the $T_{1\rho}$ minimum): In this region T_1 and T_2 are still given by Eqs. (6.12a) and (6.12b). For $T_{1\rho}$, we obtain

$$\frac{1}{T_{1\rho}} = \tfrac{3}{8}\gamma^4\hbar^2 I(I+1)\,\frac{1}{\omega_1^2\tau}\left(\sum_m \frac{A_m^{(0)}(0) - A_m^{(0)}(1)}{\overline{Z}_{\mathrm{NMR}}^{(1)}} + f(\theta,\phi)\sum_m \frac{B_m^{(0)}(0) - B_m^{(0)}(1)}{\overline{Z}_{\mathrm{NMR}}^{(1)}}\right). \tag{6.13}$$

According to Eqs. (6.12a), (6.12b), and (6.13), different orientation dependences are predicted for the three relaxation times at low temperatures.

2. *Temperature- or field-dependence of relaxation times*

For a given value of $f(\theta,\phi)$ the spectral density functions (6.5) and hence the relaxation rates (6.9) vary with the values of the parameter $\omega\tau$ as a function of the diffusion mechanism. Experimentally, a variation of $\omega\tau$ can be accomplished by both a variation of ω (i.e., the amplitude of the magnetic field) and a variation of τ (i.e., of the temperature). In principle, both types of experiments provide the same amount of information on the diffusion mechanism.

Of special interest are the shape and the width of the T_1 or $T_{1\rho}$ minimum (plotted versus the temperature) as a function of the diffusion mechanism and the crystallographic orientation of the magnetic field: no orientation dependence for high temperatures, pronounced differences in the orientation dependences of T_1, T_2, and $T_{1\rho}$ for low temperatures (see Sec. VI A 1).

B. Polycrystalline samples

In a polycrystalline sample the relaxing magnetization $M_{\mathrm{rel}}(t)$ of each individual crystallite decays towards its equilibrium value with a relaxation time $T_{\mathrm{rel}}(\theta,\phi)$ determined by its orientation relative to the magnetic field. Since generally the sum of exponentials is no exponential, in the general case simple exponential decays cannot be expected in polycrystalline samples. In Ref. 4 it was found that the magnetization then decays according to the relationship

$$\langle M_{\mathrm{rel}}(t)\rangle_{\theta,\phi} = M_0\left(\exp[-t\langle g(\theta,\phi)\rangle_{\theta,\phi}] + \sum_{n=2}^{\infty}(-1)^n\frac{t^n}{n!}\,\delta(n)\right), \tag{6.14}$$

with

$$\delta(n) = \langle g(\theta,\phi)\rangle_{\theta,\phi}^n - \langle g^n(\theta,\phi)\rangle_{\theta,\phi}. \tag{6.15}$$

TABLE I. Number of jumps $Z(|\vec{r}_m^0|)$ of spins located in the shell number z around spin i ($z=0$); $\langle x_m^0, y_m^0, z_m^0 \rangle$ denotes the permutations of the crystallographic coordinates of the atoms in shell number z ($2a_0$ is the cube edge of a unit cell; n is the number of atoms in shell z).

		bcc lattice					fcc lattice		
z	n	$\left\langle \frac{x_m^0}{a_0}, \frac{y_m^0}{a_0}, \frac{z_m^0}{a_0} \right\rangle$	$\frac{\lvert\vec{r}_m^0\rvert}{a_0}$	$Z(\lvert\vec{r}_m^0\rvert)$	z	n	$\left\langle \frac{x_m^0}{a_0}, \frac{y_m^0}{a_0}, \frac{z_m^0}{a_0} \right\rangle$	$\frac{\lvert\vec{r}_m^0\rvert}{a_0}$	$Z(\lvert\vec{r}_m^0\rvert)$
0	1	(0, 0, 0)	0	1.34	0	1	(0, 0, 0)	0	1.31
1	8	$\langle \pm 1, \pm 1, \pm 1 \rangle$	$\sqrt{3}$	0.61	1	12	$\langle 0, \pm 1, \pm 1 \rangle$	$\sqrt{2}$	0.59
2	6	$\langle 0, 0, \pm 2 \rangle$	2	0.50	2	6	$\langle 0, 0, \pm 2 \rangle$	2	0.41
3	12	$\langle 0, \pm 2, \pm 2 \rangle$	$2\sqrt{2}$	0.40	3	24	$\langle \pm 1, \pm 1, \pm 2 \rangle$	$\sqrt{6}$	0.36
4	24	$\langle \pm 1, \pm 1, \pm 3 \rangle$	$\sqrt{11}$	0.33	4	12	$\langle 0, \pm 2, \pm 2 \rangle$	$2\sqrt{2}$	0.31
5	8	$\langle \pm 2, \pm 2, \pm 2 \rangle$	$2\sqrt{3}$	0.32	5	24	$\langle 0, \pm 1, \pm 3 \rangle$	$\sqrt{10}$	0.27
6	6	$\langle 0, 0, \pm 4 \rangle$	4	0.26	6	8	$\langle \pm 2, \pm 2, \pm 2 \rangle$	$2\sqrt{3}$	0.25
7	24	$\langle \pm 1, \pm 3, \pm 3 \rangle$	$\sqrt{19}$	0.25	7	38	$\langle \pm 1, \pm 2, \pm 3 \rangle$	$\sqrt{14}$	0.22
8	24	$\langle 0, \pm 2, \pm 4 \rangle$	$2\sqrt{5}$	0.23	8	6	$\langle 0, 0, \pm 4 \rangle$	4	0.20
9	24	$\langle \pm 2, \pm 2, \pm 4 \rangle$	$2\sqrt{6}$	0.20					

$g(\theta, \phi)$ denotes the relaxation rates $1/T_1$, $1/T_2$, or $1/T_{1\rho}$, respectively, and the brackets $\langle\ \rangle$ are an abbreviation for an average over the solid angle, e.g.,

$$\langle g(\theta,\phi)\rangle_{\theta,\phi} = \frac{1}{4\pi} \int_{\theta=0}^{\pi} \int_{\phi=0}^{2\pi} g(\theta,\phi) \sin\theta \, d\theta \, d\phi \,. \tag{6.16}$$

1. Deviations from exponential decays

In this section the effect of the nonexponential part of Eq. (6.14) on the total decay of $M_{\rm rel}(t)$ will be studied in more detail. Since the relaxation rates depend on temperature (see Sec. VI A), so do $g(\theta, \phi)$ and $\delta(n)$, i.e., the relative importance of the nonexponential part of Eq. (6.14) varies with temperature. Similarly, as in Sec. VI A 1, we are going to study this effect in the following three temperature ranges:

(i) $\omega_0\tau \ll 1$, $\omega_1\tau \ll 1$ (high temperatures): According to (6.10) the three relaxation rates in this region are independent of the orientation of the magnetic field. Their temperature dependences may be written

$$1/T_{\rm rel}(\theta,\phi) \equiv g(\theta,\phi) = \alpha\tau \,, \tag{6.17}$$

where α is a constant which depends on the diffusion mechanism only. [α may be determined from

TABLE II. Values of $W_1(\vec{r}_m^0, \vec{r}_m^*)$ (which are greater than 1%) for one nearest neighbor of spin i (located at $\vec{r}_m^0$).

	bcc lattice				fcc lattice		
$\vec{r}_m^0 = \left(\frac{x_m^0}{a_0}, \frac{y_m^0}{a_0}, \frac{z_m^0}{a_0}\right)$	$\vec{r}_m^* = \left(\frac{x_m^*}{a_0}, \frac{y_m^*}{a_0}, \frac{z_m^*}{a_0}\right)$	$W_1(\vec{r}_m^0, \vec{r}_m^*)$[%]	$\vec{r}_m^0 = \left(\frac{x_m^0}{a_0}, \frac{y_m^0}{a_0}, \frac{z_m^*}{a_0}\right)$	$\vec{r}_m^* = \left(\frac{x_m^*}{a_0}, \frac{y_m^*}{a_0}, \frac{z_m^*}{a_0}\right)$	$W_1(\vec{r}_m^0, \vec{r}_m^*)$[%]
	(0, 0, 0)	11.8		(0, 0, 0)	8.1
	(−1, −1, −1)	7.7		(−1, 0, −1)	6.2
	(−1, −1, 1)	7.4		(−1, 1, 0)	5.6
	(−1, 1, −1)	7.4		(0, 1, −1)	5.8
	(−1, 1, 1)	7.6		(−1, −1, 0)	5.5
	(1, −1, −1)	7.5		(−1, 0, 1)	5.9
	(1, −1, 1)	7.1		(0, −1, −1)	5.9
(1, 1, 1)	(1, 1, −1)	7.5	(1, 1, 0)	(0, 1, 1)	5.9
	(1, 1, 1)	7.2		(1, 0, −1)	6.0
	(0, 0, 2)	1.5		(1, 1, 0)	5.4
	(0, −2, 0)	3.4		(0, −1, 1)	5.8
	(2, 0, 0)	1.6		(1, −1, 0)	5.6
	(0, 2, 0)	1.7		(1, 0, 1)	5.8
	(0, 0, −2)	3.3		(−2, 0, 0)	1.8
	(−2, 0, 0)	3.0		(0, −2, 0)	1.8
	(−2, 0, −2)	2.2		(−2, −1, 1)	1.2
	(0, −2, −2)	2.3		(−1, −2, −1)	1.3
	(−2, −2, 0)	2.3		(−1, −2, 1)	1.3

TABLE III. Lattice sums for $s=0$ and $s=1$ in units of a_0^{-6} ($2a_0$ is the cube edge of a unit cell); see, e.g., Eqs. (6.7) and (6.8).

bcc lattice

s	q	$\sum_m \frac{A_m^{(q)}(s)}{\bar{Z}^{(1)}_{\mathrm{NMR}}}$	$\sum_m \frac{B_m^{(q)}(s)}{\bar{Z}^{(1)}_{\mathrm{NMR}}}$	$\sum_m A_m^{(q)}(s)\,\bar{Z}^{(1)}_{\mathrm{NMR}}$	$\sum_m B_m^{(q)}(s)\,\bar{Z}^{(1)}_{\mathrm{NMR}}$
	0	0.1291	0.0789	0.4200	0.3315
0	1	0.0392	−0.0088	0.1433	−0.0368
	2	0.1212	0.0088	0.4271	0.0368
	0	0.0380	0.0063	0.1107	0.0272
1	1	0.0079	−0.0007	0.0249	−0.0030
	2	0.0285	0.0007	0.0873	0.0030

fcc lattice

s	q	$\sum_m \frac{A_m^{(q)}(s)}{\bar{Z}^{(1)}_{\mathrm{NMR}}}$	$\sum_m \frac{B_m^{(q)}(s)}{\bar{Z}^{(1)}_{\mathrm{NMR}}}$	$\sum_m A_m^{(q)}(s)\,\bar{Z}^{(1)}_{\mathrm{NMR}}$	$\sum_m B_m^{(q)}(s)\,\bar{Z}^{(1)}_{\mathrm{NMR}}$
	0	0.5913	0.2354	1.9629	0.8938
0	1	0.1509	−0.0262	0.5255	−0.0993
	2	0.4994	0.0262	1.7040	0.0993
	0	0.1194	0.0296	0.3180	0.1139
1	1	0.0264	−0.0033	0.0779	−0.0126
	2	0.0921	0.0033	0.2598	0.0126

TABLE V. Orientation dependence of the relaxation times on the low-temperature side of the T_1 minimum. [$\alpha = \frac{3}{2}\gamma^4\hbar^2 I(I+1)$, and $f(\theta,\phi)$ is given by Eq. (6.6); see Eqs. (6.12) and (6.13) and Table IV].

bcc lattice

	$\omega_0\tau \gg 1,\ \omega_1\tau \ll 1$	$\omega_0\tau \gg 1,\ \omega_1\tau \gg 1$
$\frac{1}{T_{1\rho}}$	$[0.1915 + 0.0939\, f(\theta,\phi)]\,\frac{\alpha\tau}{a_0^6}$	$[0.0228 + 0.0182\, f(\theta,\phi)]\,\frac{\alpha}{\omega_1^2\tau a_0^6}$
$\frac{1}{T_2}$	$[0.1915 + 0.0939\, f(\theta,\phi)]\,\frac{\alpha\tau}{a_0^6}$	
$\frac{1}{T_1}$	$[0.2179 - 0.0243\, f(\theta,\phi)]\,\frac{\alpha}{\omega_0^2\tau a_0^6}$	

fcc lattice

	$\omega_0\tau \gg 1,\ \omega_1\tau \ll 1$	$\omega_0\tau \gg 1,\ \omega_1\tau \gg 1$
$\frac{1}{T_{1\rho}}$	$[0.7526 + 0.2624\, f(\theta,\phi)]\,\frac{\alpha\tau}{a_0^6}$	$[0.1180 + 0.0515\, f(\theta,\phi)]\,\frac{\alpha}{\omega_1^2\tau a_0^6}$
$\frac{1}{T_2}$	$[0.7526 + 0.2624\, f(\theta,\phi)]\,\frac{\alpha\tau}{a_0^6}$	
$\frac{1}{T_1}$	$[0.9056 - 0.0687\, f(\theta,\phi)]\,\frac{\alpha}{\omega_0^2\tau a_0^6}$	

comparison of Eqs. (6.17) and (6.10).]

From Eqs. (6.17) and (6.15), we find

$$\delta(n) = 0 \tag{6.18}$$

for arbitrary n, and with Eq. (6.14),

$$\langle M_{\mathrm{rel}}(t)\rangle_{\theta,\phi} = M_0 \exp[-t\langle g(\theta,\phi)\rangle_{\theta,\phi}]\,. \tag{6.19}$$

Equation (6.19) predicts simple exponential relaxation functions for polycrystals at high temperature, with the relaxation times $\langle 1/T_1\rangle_{\theta,\phi}$, $\langle 1/T_2\rangle_{\theta,\phi}$, and $\langle 1/T_{1\rho}\rangle_{\theta,\phi}$, respectively.

(ii) $\omega_0\tau \gg 1$, $\omega_1\tau \ll 1$ (medium temperatures): For the spin-lattice relaxation rate we can write [see Eq. (6.12a)]

$$1/T_1 \equiv g(\theta,\phi) = \frac{\alpha_1}{\omega_0^2\tau}\,[\beta_1 + \gamma_1 f(\theta,\phi)], \tag{6.20}$$

where α_1, β_1, and γ_1 are constants which can be determined from the comparison of Eqs. (6.20) and (6.12a). Inserting Eq. (6.20) into (6.15), we get

$$\delta(n) = \frac{\alpha_1^n}{\omega_0^{2n}\tau^n}\left[\langle(\beta_1 + \gamma_1 f(\theta,\phi))^n\rangle_{\theta,\phi} - \langle(\beta_1 + \gamma_1 f(\theta,\phi))^n\rangle_{\theta,\phi}\right], \tag{6.21}$$

and from Eq. (6.14),

$$\langle M_{\parallel}(t)\rangle_{\theta,\phi} = M_0\left[\exp\left(-\frac{\alpha_1 t}{\omega_0^2\tau}\langle\beta_1 + \gamma_1 f(\theta,\phi)\rangle_{\theta,\phi}\right) + \sum_{n=2}^{\infty}(-1)^n\frac{t^n}{n!}\frac{C_1(n)}{\omega_0^{2n}\tau^n}\right], \tag{6.22}$$

where $C_1(n)$ is constant for a given value of n and $M_{\parallel}(t)$ denotes the magnetization parallel to $\vec{H}_0$.

Analogously to the derivation of Eq. (6.22), we obtain for the magnetization $M_{\perp}$ perpendicular to $\vec{H}_0$ (which decays to zero),

TABLE IV. Prefactors determining the orientation dependences of the spectral density functions and of the relaxation times for $\omega\tau \gg 1$ [see Eqs. (6.7), (6.12), and (6.13)] and for $\omega\tau \ll 1$ [See Eqs. (6.8) and (6.10)] in units of a_0^{-6}.

bcc lattice

q	$\sum_m \frac{A_m^{(q)}(0) - A_m^{(q)}(1)}{\bar{Z}^{(1)}_{\mathrm{NMR}}}$	$\sum_m \frac{B_m^{(q)}(0) - B_m^{(q)}(1)}{\bar{Z}^{(1)}_{\mathrm{NMR}}}$	$\sum_{s=0}^{25}\sum_m A_m^{(q)}(s)\,\bar{Z}^{(s)}_{\mathrm{NMR}}$	$\sum_{s=0}^{25}\sum_m B_m^{(q)}(s)\,\bar{Z}^{(s)}_{\mathrm{NMR}}$
0	0.0911	0.0726	0.7658	0.3756
1	0.0313	−0.0081	0.2112	−0.0417
2	0.0927	0.0081	0.6782	0.0417

fcc lattice

q	$\sum_m \frac{A_m^{(q)}(0) - A_m^{(q)}(1)}{\bar{Z}^{(1)}_{\mathrm{NMR}}}$	$\sum_m \frac{B_m^{(q)}(0) - B_m^{(q)}(1)}{\bar{Z}^{(1)}_{\mathrm{NMR}}}$	$\sum_{s=0}^{20}\sum_m A_m^{(q)}(s)\,\bar{Z}^{(s)}_{\mathrm{NMR}}$	$\sum_{s=0}^{20}\sum_m B_m^{(q)}(s)\,\bar{Z}^{(s)}_{\mathrm{NMR}}$
0	0.4719	0.2058	3.0103	1.0507
1	0.1245	−0.0229	0.7301	−0.1167
2	0.4073	0.0229	2.4613	0.1167

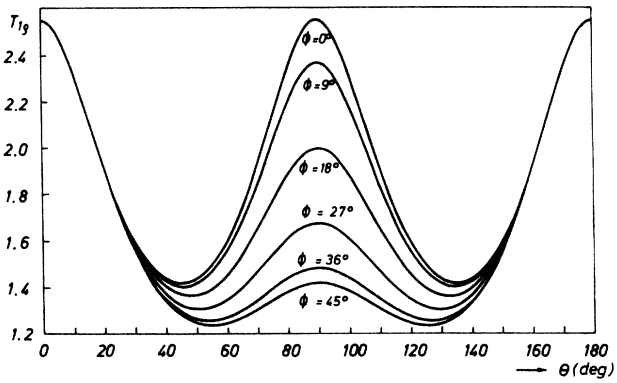

FIG. 4. Variation of $T_{1\rho}$ for $\omega_0\tau \gg 1$ and $\omega_1\tau \gg 1$ between $\theta = 0$ and $\theta = 180°$ for different values of ϕ for a bcc lattice in arbitrary units [see Eq. (6.13) and Table V].

$$\langle M_\perp(t)\rangle_{\theta,\phi} = M_0\Big(\exp[-\alpha_2 t\langle\beta_2 + \gamma_2 f(\theta,\phi)\rangle_{\theta,\phi}\tau] + \sum_{n=2}^{\infty}(-1)^n\frac{t^n}{n!}C_2(n)\tau^n\Big). \quad (6.23)$$

For decreasing temperature (increasing values of $\omega\tau$) the exponential in Eq. (6.22) increases, while the individual terms of the nonexponential part decrease very fast. The opposite is true in Eq. (6.23): with decreasing temperature the nonexponential part increases while the exponential part decreases. We may thus conclude that the lower the temperature the greater are the deviations of the T_2 decay from a simple exponential and the smaller are the deviations in the T_1 decay. This point of view is also supported by the dependence of $M_\parallel(t)$ and $M_\perp(t)$ on ω_0: increasing ω_0 should result in the exponential part of $M_\parallel(t)$ to increase relative to the nonexponential terms, while no effect should be observed in the decay of $M_\perp(t)$ [see Eqs. (6.22) and (6.23)].

This suggests a new method to determine diffusion mechanisms in polycrystalline samples: Assuming that a simple exponential decay of $M_\perp(t)$ is observed in a single crystal at temperatures below the T_1 minimum, deviations from this simple behavior, which are characteristic for the diffusion mechanism, are predicted for polycrystalline samples from Eq. (6.23).

Relationships similar to Eqs. (6.22) and (6.23) can easily be derived for the $T_{1\rho}$ decay on both sides of the $T_{1\rho}$ minimum. It can be shown that the deviations from a simple exponential decay are not as significant as in the T_2 decay discussed above.

2. *Shape of the T_1 and $T_{1\rho}$ minimum*

In polycrystalline samples the effect of the crystallographic orientation of the magnetic field on the shape of the T_1 or $T_{1\rho}$ minimum versus temperature (as discussed in Sec. VI A 2) is averaged out. Nevertheless, there is a significant effect of the diffusion mechanism on the symmetry properties and the width of these minima. This can be seen as following.

Let us assume that the exponential part is dominant in the relaxation equations describing the decay of nonequilibrium magnetizations, which were derived in Sec. VI B 1. Then we can write

$$\langle M_{\mathrm{rel}}(t)\rangle_{\theta,\phi} = M_0\exp\Big(-t\Big\langle\frac{1}{T_{\mathrm{rel}}(\theta,\phi)}\Big\rangle_{\theta,\phi}\Big). \quad (6.24)$$

The averaged relaxation rates $\langle 1/T_{\mathrm{rel}}(\theta,\phi)\rangle_{\theta,\phi}$ can

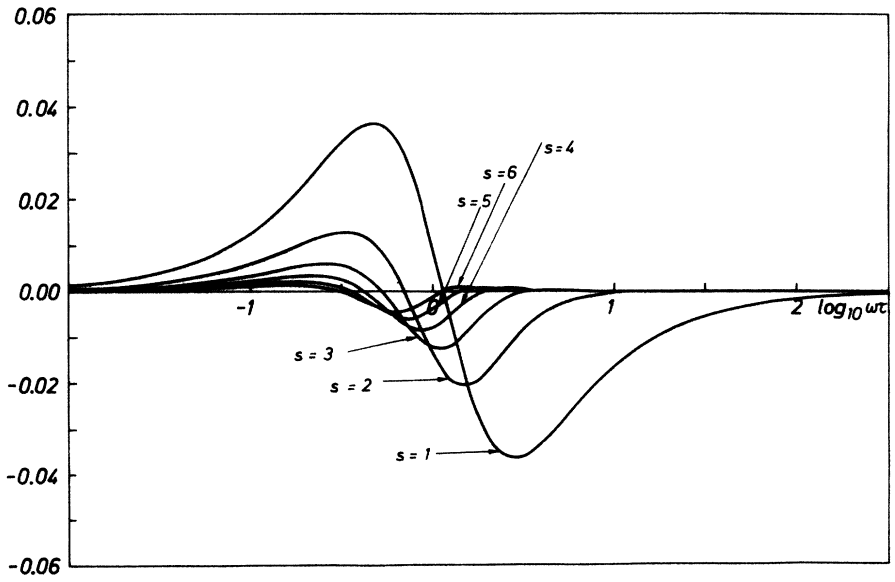

FIG. 5. Individual terms of the summation over s in Eq. (6.26) for $s=1$ to $s=6$ in units of $a_0^{-6}\omega^{-1}$ for a bcc-lattice ($2a_0$ is the cube edge of a unit cell).

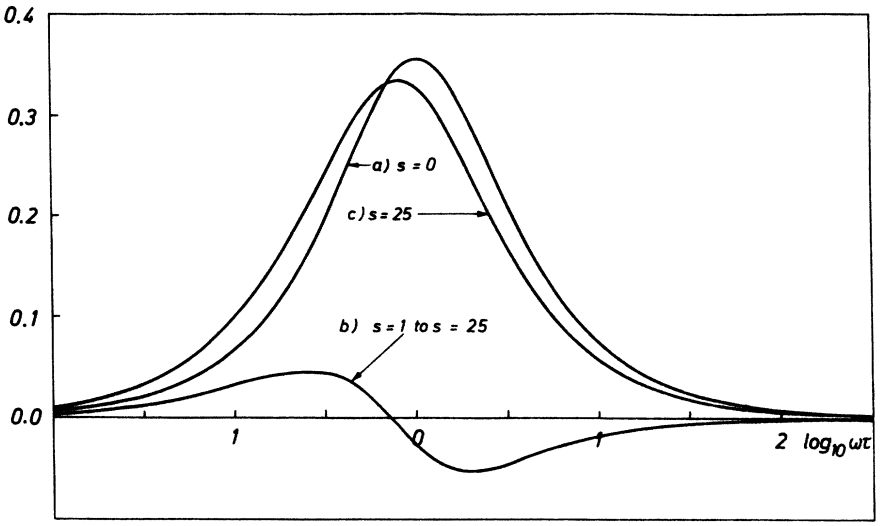

FIG. 6. Curve (a) shows the first term ($s=0$) of the sum (6.26) for $q=0$. Curve (b) demonstrates the effect of terms $s>0$ on the leading term. The sum of (a) and (b) is shown in curve c) (in units of $\omega^{-1}a_0^{-6}$).

easily be derived from Eqs. (6.9a)–(6.9c) since they may be written in terms of the averaged spectral density functions $\langle \mathcal{J}^{(q)}(\omega)\rangle_{\theta,\phi}$. Using the relationship[4]

$$\langle f(\theta,\phi)\rangle_{\theta,\phi}=0.8\ , \tag{6.25}$$

we obtain, from Eq. (6.5),

$$\langle \mathcal{J}^{(q)}(\omega)\rangle_{\theta,\phi}=\frac{1}{\omega}\sum_m\sum_{s=0}^{\infty} j_s(\omega\tau_{\mathrm{NMR}}^{(s)})\left[A_m^{(q)}(s)+0.8\,B_m^{(q)}(s)\right]\ . \tag{6.26}$$

From Eq. (6.26) we see that the main effect of the diffusion mechanism on the shape of $\mathcal{J}^{(q)}(\omega)$ vs $\omega\tau$ is due to the relative shift on the $\omega\tau$ scale of the individual terms in the summation over s. This is a result of the change of the pair correlation (and hence of the number of relative jumps per encounter) with the number s of encounters [see Eq. (4.2) and Sec. IV A). Also, the prefactors of the individual terms in the summation over s depend on the diffusion mechanism.

VII. NUMERICAL RESULTS FOR DIFFUSION VIA SINGLE VACANCIES IN CUBIC CRYSTALS

As shown so far in this paper, the effect of a defect diffusion mechanism on nuclear magnetic relaxation can be characterized by a few parameters, which are related to the rearrangement resulting from one encounter with the randomly migrating defect. For diffusion via monovacancies in Sec. VII A we shall outline a method for the numerical determination of the probabilities $E_s(\vec{r}_m^{\,0}, \vec{r}_m)$ and the number of correlated jumps $Z(\vec{r}_m^{\,0})$, from which the quantities $W_s(\vec{r}_m^{\,0}, \vec{r}_m)$ and $\tau_{\mathrm{NMR}}^{(s)}$ and thus their effect on the relaxation properties described in Sec. VI can be calculated (Secs. VII B and VII C).

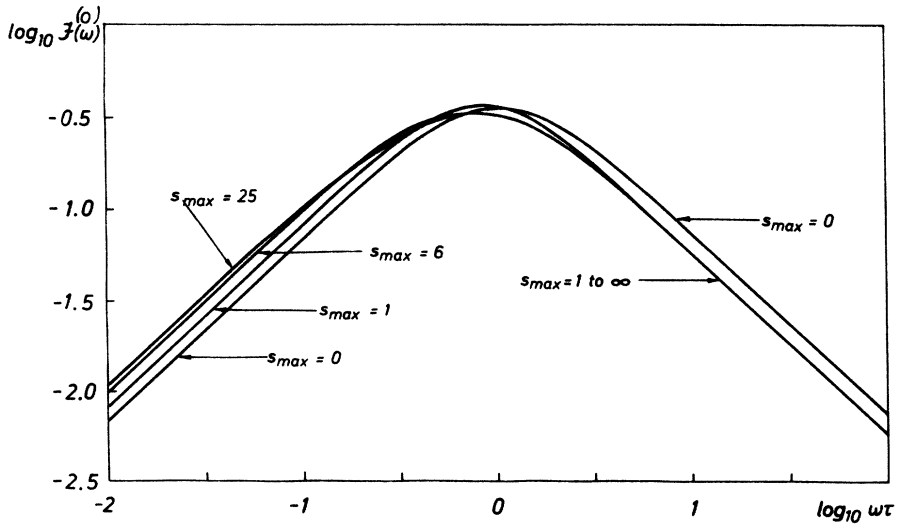

FIG. 7. $\log_{10}\mathcal{J}^{(0)}(\omega)$ vs $\log_{10}\omega\tau$. The upper limit of the summation over s in Eq. (6.26) was taken as $s_{\max}=0, 1, 6$, and 25 (in units of $\omega^{-1}a_0^{-6}$).

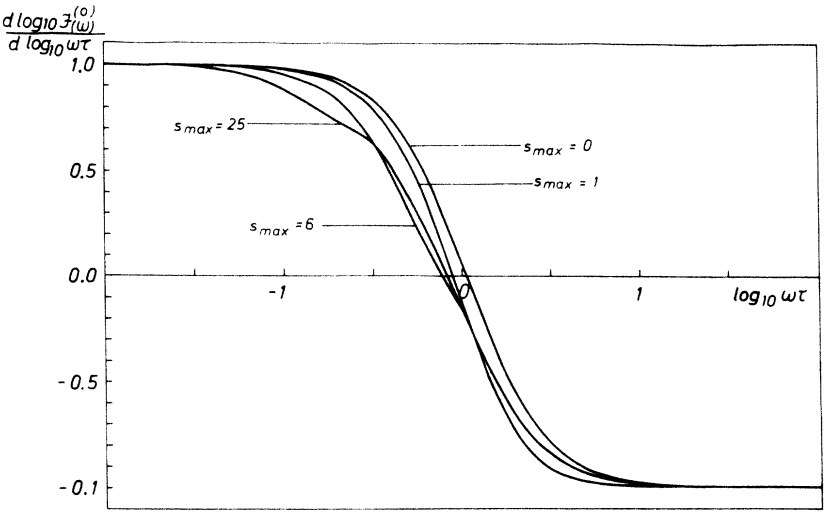

FIG. 8. First derivatives of the curves shown in Fig. 7.

A. Computer simulation of the random migration of a vacancy

The so-called Monte Carlo method (see, e.g. Ref. 6) allows the random migration of a vacancy to be simulated on a computer equipped with a procedure for the generation of random numbers.

The moment at which the vacancy has caused the first jump of spin i to the nearest-neighbor site g is denoted by $t' = 0$. Before this initial jump of i (i.e., for $t' < 0$), the vacancy has approached site g from, say, infinity and, on its way, has caused jumps of spins m in the surroundings of i. This situation for $t' < 0$ is simulated by letting the vacancy start its random walk at the lattice site g with the restriction that no jump of spin i may be caused (i.e., the time scale for vacancy jumps is reversed). The probabilities $B_g^b(\vec{r}_m^0, \vec{r}_m')$ that spin m has jumped from $\vec{r}_m^0$ to $\vec{r}_m'$ *before* the first jump of i are obtained from repreated simulation (e.g., 1000 times) of this restricted motion of the vacancy.

In the simulation for $t' > 0$ the vacancy starts at the origin (spin i now is located at site g), and the vacancy may migrate through the crystal without restrictions. Thus we obtain the probabilities $B_g^a(\vec{r}_m', \vec{r}_m)$, that *after* the first jump of i spin m has jumped from $\vec{r}_m'$ to $\vec{r}_m$, and $B_g(0, \vec{r}_i)$ that spin i is located at $\vec{r}_i$ after the vacancy has left the surroundings of i.

From the relationship

$$B_g(\vec{r}_m^0, \vec{r}_m) = \sum_{\vec{r}_m'} B_g^b(\vec{r}_m^0, \vec{r}_m')\, B_g^a(\vec{r}_m', \vec{r}_m), \qquad (7.1)$$

we obtain the probability $B_g(\vec{r}_m^0, \vec{r}_m)$ that a spin m jumped from $\vec{r}_m^0$ to $\vec{r}_m$, while the vacancy actually rearranged the surroundings of spin i. Because of symmetry reasons it is sufficient to determine $B_g(\vec{r}_m^0, \vec{r}_m)$ in the way described above for one specific value of g only, from which the probabilities for the other values of g may be obtained by simple symmetry transformations.

Similarly, the mean number of jumps is obtained from the simulation. For both the *fcc* and the *bcc* lattice the jumps of about 140 atoms to more than 300 lattice sites around spin i were taken into account during the simulation of 1000 encounters.

TABLE VI. Relaxation times for polycrystalline samples on the low-temperature side and on the high-temperature side of the T_1 minimum $[\alpha = \frac{3}{2}\gamma^4\hbar^2 I(I+1)]$.

	bcc lattice				fcc lattice		
	$\omega_0\tau \gg 1$ $\omega_0\tau \ll 1$	$\omega_0\tau \gg 1$ $\omega_1\tau \gg 1$	$\omega_0\tau \ll 1$		$\omega_0\tau \gg 1$ $\omega_0\tau \ll 1$	$\omega_0\tau \gg 1$ $\omega_1\tau \gg 1$	$\omega_0\tau \ll 1$
$\left\langle \frac{1}{T_{1\rho}} \right\rangle_{\theta,\phi}$	$0.2656\,\frac{\alpha\tau}{a_0^6}$	$0.0374\,\frac{\alpha}{\omega_1^2\tau a_0^6}$	$0.8894\,\frac{\alpha\tau}{a_0^6}$	$\left\langle \frac{1}{T_{1\rho}} \right\rangle_{\theta,\phi}$	$0.9625\,\frac{\alpha\tau}{a_0^6}$	$0.1592\,\frac{\alpha}{\omega_1^2\tau a_0^6}$	$3.1920\,\frac{\alpha\tau}{a_0^6}$
$\left\langle \frac{1}{T_2} \right\rangle_{\theta,\phi}$	$0.2656\,\frac{\alpha\tau}{a_0^6}$		$0.8894\,\frac{\alpha\tau}{a_0^6}$	$\left\langle \frac{1}{T_2} \right\rangle_{\theta,\phi}$	$0.9628\,\frac{\alpha\tau}{a_0^6}$		$3.1920\,\frac{\alpha\tau}{a_0^6}$
$\left\langle \frac{1}{T_1} \right\rangle_{\theta,\phi}$	$0.1985\,\frac{\alpha}{\omega_0^2\tau a_0^6}$		$0.8894\,\frac{\alpha\tau}{a_0^6}$	$\left\langle \frac{1}{T_1} \right\rangle_{\theta,\phi}$	$0.8506\,\frac{\alpha}{\omega_0^2\tau a_0^6}$		$3.1920\,\frac{\alpha\tau}{a_0^6}$

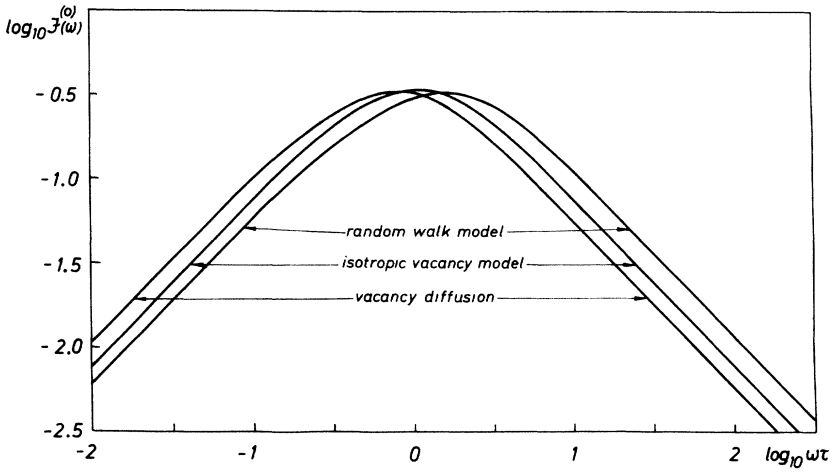

FIG. 9. Doubly logarithmic plot of $\mathcal{J}(0)(\omega)$ vs $\omega\tau$ for a random-walk diffusion mechanism (Ref. 4), vacancy diffusion (present model), and for the so-called isotropic vacancy model (Ref. 3), in which pair correlations were neglected (in units of $\omega^{-1}a_0^{-6}$).

Seven hundred vacancy jumps *before* the first jump of i and the same number *after* it proved to be sufficient to get satisfying accuracy of the values of $B_g(\vec{r}_m^0, \vec{r}_m)$.

With the numerical values of $B_g(\vec{r}_m^0, \vec{r}_m)$ and $Z_g(\vec{r}_m^0)$ thus obtained, $W_1(\vec{r}_m^0, \vec{r}_m^*)$, and $Z(\vec{r}_m^0)$ were determined from Eqs. (4.10a) and (3.2) for the fcc and the bcc lattice. The relations (3.1a), (3.1b), and (4.10b) were used to check the numerical values.

To get an idea of the magnitude of these quantities some selected values are listed in the Tables I and II.

B. Numerical results for single crystals

Using the results of Sec. VII A the probabilities $W_s(\vec{r}_m^0, \vec{r}_m^*)$ and the time $\tau_{\mathrm{NMR}}^{(s)}$ can be calculated using the procedure described in Sec. IV B. In this way the lattice sums in Eq. (6.7) and (6.8) have been evaluated for the fcc and the bcc lattice. The terms for $s=0$ and $s=1$ are shown in Table III.

In all summations over m the 1331 closest spins were taken into account. The summation over s, the number of encounters, was extended from $s=0$ to $s_{\max}=25$ (bcc lattice) and to $s_{\max}=20$ (fcc lattice) in order to obtain sufficient convergence on the high-temperature side of the maxima of $\mathcal{J}^{(q)}(\omega)$. The results obtained in this way are listed in Table IV.

In Sec. VI A 1 it was derived that for temperatures above the T_1 minimum (i.e., for $\omega_0\tau \ll 1$) T_1, T_2, and $T_{1\rho}$ are expected to be independent of the orientation of $\vec{H}_0$. The orientation dependence on the low-temperature side of the T_1 minimum ($\omega_0\tau \gg 1$) is readily obtained from Table IV and the relations (6.12) and (6.13). Thus, we get the values listed in Table V.

The typical dependence of the relaxation times on the angles θ and ϕ in the low-temperature region (listed in Table V) is shown in Fig. 4, where $T_{1\rho}$ is plotted versus θ for different values of ϕ.

As we see from Fig. 4 the periodicity of $T_{1\rho}$ as a function of θ is $\frac{1}{2}\pi$ for $\phi=0$ (field in the x-z plane) but π for $\phi\neq 0$ [see also Eq. (6.6)].

In Sec. VI A 2 it was shown that the shape of the T_1 or $T_{1\rho}$ minimum plotted versus temperature is a function of the crystallographic orientation of the magnetic field and of the diffusion mechanism. As shown in Sec. VI B 2 also in polycrystalline samples the second effect can be observed. Therefore the shapes of the two minima will be studied in some detail for polycrystalline samples only (Sec. VII C), while the orientation dependence of these shapes is not pursued in further detail in this paper.

C. Numerical results for polycrystalline samples

The deviations from exponential decays as described in Sec. VI B 1 have not been studied numerically. In the present section we investigate the shape of the intensity functions (6.26) versus $\omega\tau$ in some detail. Therefore, we assume that experimentally exponential decays have been found which are characterized by the relaxation rates $\langle 1/T_1\rangle_{\theta,\phi}$, $\langle 1/T_2\rangle_{\theta,\phi}$, or $\langle 1/T_{1\rho}\rangle_{\theta,\phi}$. According to Sec. VI B 2 these relaxation rates are linear combinations of the intensity functions $\langle \mathcal{J}^{(q)}(\omega)\rangle_{\theta,\phi}$.

In Fig. 5 the terms $s=1$ to $s=6$ of Eq. (6.26) have been plotted versus $\log_{10}\omega\tau$. The effect of all terms $s>0$ on the leading term of Eq. (6.26) is shown in Fig. 6. In order to demonstrate the convergence of the summation over s in (6.26), in Fig. 7 the upper limit of the s sum has been varied from $s_{\max}=0$ to $s_{\max}=25$.

The effect of higher-order s terms on the shape of $\mathcal{J}^{(q)}(\omega)$ is best demonstrated by a plot of the first derivatives of the curves shown in Fig. 7. From Fig. 8 it is seen that the asymmetry of $\mathcal{J}^{(0)}(\omega)$ with respect to that value of $\omega\tau$ for which $\mathcal{J}^{(0)}(\omega)$ shows a maximum is caused by the higher-order s terms.

With these results for the spectral-density functions and from the results of Sec. VII B the relaxation rates for polycrystalline samples may be calculated for a given value of $\omega\tau$. Table VI shows the numerical values in the regions $\omega_0\tau \gg 1$ and $\omega_0\tau \ll 1$ respectively.

VIII. DISCUSSION

The only model which has so far been available to describe the orientation dependence of the high-field relaxation rates is Torrey's random-walk model[2] treated in Ref. 4. In Sec. V this model was shown to be included in the present theory as the limiting case of uncorrelated diffusion.

Although the absolute values of the relaxation rates predicted for a monovacancy mechanism on the one hand, and random-walk diffusion on the other, differ considerably (20–30%), a comparison of the variation of the relaxation rates with the crystallographic orientation of the field $\vec{H}_0$ shows only small differences between the two models (see Ref. 4 and Sec. VII B). Thus we find, e.g., a variation of 49% of $1/T_2$ for vacancy diffusion instead of 44% for the random-walk model. The differences in $1/T_{1\rho}$ are even smaller (80% instead of 82%).

Considerable differences, however, are predicted in the shapes of the spectral density functions (and hence of the relaxation rates) as a function of $\log_{10}\omega\tau$. Figure 9 shows plots of $\mathcal{J}^{(0)}(\omega)$ for the present model (monovacancies), the random walk model of diffusion (Ref. 4), and the so-called "isotropic-vacancy model"[3] (see also Sec. I).

From Fig. 9 it is found that the width of the maximum of $\mathcal{J}^{(0)}(\omega)$ is substantially smaller for vacancy diffusion than for random-walk diffusion. The reason is that because of the pair correlations the individual s terms in Eq. (6.26) are shifted relative to one another on the $\omega\tau$ scale, since the number of relative jumps per encounter varies with the number of encounters of the two spins of a pair. This narrowing effect on the shape of $\mathcal{J}^{(q)}(\omega)$ deduced for random-walk diffusion seems to be a general feature of correlated diffusion mechanisms.

ACKNOWLEDGMENTS

The author would like to thank Professor A. Seeger, Dr. H. Mehrer, and Dr. E. Cavelius for numerous helpful discussions.

[1]M. Eisenstadt and A. G. Redfield, Phys. Rev. 132, 635 (1963).
[2]H. C. Torrey, Phys. Rev. 92, 962 (1953).
[3]D. Wolf, Z. Naturforsch A 26, 1816 (1971).
[4]D. Wolf, J. Magn. Res. (to be published).
[5]A. Abragam, *The Principles of Nuclear Magnetism* (Clarendon, Oxford, 1961).
[6]H. Mehrer, Z. Naturforsch. A 24, 358 (1969).